JCI The Journal of Clinical Investigation

Blockade of T cell costimulation reveals interrelated actions of CD4+ and CD8+ T cells in control of SIV replication

David A. Garber, … , Silvija I. Staprans, Mark B. Feinberg

J Clin Invest. 2004;113(6):836-845. https://doi.org/10.1172/JCI19442.

Article AIDS/HIV

In vivo blockade of CD28 and CD40 T cell costimulation pathways during acute simian immunodeficiency virus (SIV) infection of rhesus macaques was performed to assess the relative contributions of $CD4^+$ T cells, $CD8^+$ T cells, and Ab responses in modulating SIV replication and disease progression. Transient administration of CTLA4-Ig and anti–CD40L mAb to SIV-infected rhesus macaques resulted in dramatic inhibition of the generation of both SIV-specific cellular and humoral immune responses. Acute levels of proliferating $CD8^+$ T cells were associated with early control of SIV viremia but did not predict ensuing set point viremia or survival. The level of in vivo $CD4^+$ T cell proliferation during acute SIV infection correlated with concomitant peak levels of SIV plasma viremia, whereas measures of in vivo $CD4^+$ T cell proliferation that extended into chronic infection correlated with lower SIV viral load and increased survival. These results suggest that proliferating $CD4^+$ T cells function both as sources of virus production and as antiviral effectors and that increased levels of $CD4^+$ T cell proliferation during SIV infections reflect antigen-driven antiviral responses rather than a compensatory homeostatic response. These results highlight the interrelated actions of $CD4^+$ and $CD8^+$ T cell responses in vivo that modulate SIV replication and pathogenesis.

 Related Commentary, page 808

Blockade of T cell costimulation reveals interrelated actions of CD4+ and CD8+ T cells in control of SIV replication

David A. Garber,[1] Guido Silvestri,[1,2] Ashley P. Barry,[1] Andrew Fedanov,[1] Natalia Kozyr,[1] Harold McClure,[3] David C. Montefiori,[4] Christian P. Larsen,[5] John D. Altman,[1,6] Silvija I. Staprans,[1,2,6] and Mark B. Feinberg[1,2,6]

[1]Emory Vaccine Center, [2]Department of Medicine, and [3]Yerkes National Primate Research Center, Emory University, Atlanta, Georgia, USA. [4]Department of Surgery, Duke University Medical Center, Durham, North Carolina, USA. [5]Department of Surgery and [6]Department of Microbiology & Immunology, Emory University, Atlanta, Georgia, USA.

In vivo blockade of CD28 and CD40 T cell costimulation pathways during acute simian immunodeficiency virus (SIV) infection of rhesus macaques was performed to assess the relative contributions of CD4+ T cells, CD8+ T cells, and Ab responses in modulating SIV replication and disease progression. Transient administration of CTLA4-Ig and anti–CD40L mAb to SIV-infected rhesus macaques resulted in dramatic inhibition of the generation of both SIV-specific cellular and humoral immune responses. Acute levels of proliferating CD8+ T cells were associated with early control of SIV viremia but did not predict ensuing set point viremia or survival. The level of in vivo CD4+ T cell proliferation during acute SIV infection correlated with concomitant peak levels of SIV plasma viremia, whereas measures of in vivo CD4+ T cell proliferation that extended into chronic infection correlated with lower SIV viral load and increased survival. These results suggest that proliferating CD4+ T cells function both as sources of virus production and as antiviral effectors and that increased levels of CD4+ T cell proliferation during SIV infections reflect antigen-driven antiviral responses rather than a compensatory homeostatic response. These results highlight the interrelated actions of CD4+ and CD8+ T cell responses in vivo that modulate SIV replication and pathogenesis.

Introduction

The mechanisms by which host immune responses may control immunodeficiency virus replication and why they almost invariably fail to prevent progression to AIDS remain incompletely understood. Acute HIV infection of humans and simian immunodeficiency virus (SIV) infection of rhesus macaques are characterized by a transient peak in viremia, the partial resolution of which correlates temporally with the emergence of virus-specific CD8+ T cell and Ab responses (1–4). The resulting set point level of viremia is a robust predictor of the ensuing rate of progression to AIDS in both HIV-infected humans (5) and SIV-infected macaques (6–8). Observations of several host-virus interactions during primary HIV (or SIV) infection suggest that acute virus-specific CD8+ T cell responses can regulate (at least partially) the extent of virus replication. These interactions include temporal correlations between CD8+ T cell responses and initial decline in acute viremia (1–4) and the emergence of CTL-escape mutants during acute infection (9–11). In addition, Ab-mediated depletion of CD8α+ cells during both primary and chronic SIV infection of rhesus macaques results in significant increases in SIV replication and has been interpreted as evidence for antiviral regulation of SIV replication by SIV-specific CD8+ T cells (12–14). The observed increases in SIV viremia reported in these CD8α+ depletion studies, however, potentially derive from factors in addition to the loss of SIV-specific CD8+ T cell–mediated antiviral control. These factors include global depletion of CD8α+ T cell subsets with ensuing disruption of overall lymphocyte homeostasis, activation of CD4+ T cells in response to bolus injections of xenogenic and antigenic CD8α-depleting Ab's, depletion of CD8α+ NK cells (a cell population that plays an important role in innate immune responses and that proliferates in response to acute SIV infection) (15), and potential reactivation of latent infectious agents (e.g., CMV) that result in increased levels of CD4+ T cell activation. Thus, the quantitative contribution of virus-specific CD8+ T cell responses toward control of acute and chronic immunodeficiency virus replication remains largely unknown. Furthermore, in contrast to models of CD8+ T cell regulation of acute immunodeficiency virus replication, it has been theorized that the kinetics of acute HIV replication can be wholly explained by exhaustion of the supply of CD4+ target cells that produce virus, independent of antiviral immune responses (16).

We sought to experimentally induce SIV antigen-specific tolerance in vivo, without disruption of lymphocyte homeostasis or unintentional depletion of other cell types, in order to assess the relative contributions of CD4+ target cells, antigen-specific CD4+ Th and CD8+ T cells, and virus-specific Ab's to the dynamics of acute SIV replication. Toward this end, we have used in vivo administration of CTLA4-Ig and anti-CD40L mAb during acute SIV infection of rhesus macaques to achieve costimulation (CS) blockade of SIV antigen-specific T and B cell responses. CTLA4-Ig (17) and anti-CD40L mAb block CD28-CD80/86 and CD40-CD40L lymphocyte-signaling pathways, respectively, that are required for the generation of primary T and T-dependent B lymphocyte responses (18–21). CTLA4-Ig is a soluble form of the extracellular domain of human CTLA4, which binds CD80/86 on APCs with high avidity and suppresses T

Nonstandard abbreviations used: area under the curve (AUC); costimulation (CS); enzyme-linked immunosorbent spot (ELISPOT); germinal center (GC); simian immunodeficiency virus (SIV).

Conflict of interest: The authors have declared that no conflict of interest exists.

Citation for this article: *J. Clin. Invest.* **113**:836–845 (2004). doi:10.1172/JCI200419442.

cell–dependent Ab responses against foreign antigens in mice (22, 23). Anti-CD40L mAb prevents CD40-CD40L interactions between $CD4^+$ T cells and B cells. These interactions are essential for development of antigen-specific humoral immune responses, including activation and differentiation of B cells, immunoglobulin class switching, formation of B cell germinal centers in lymph nodes, and development of B cell memory (24). In addition, CD40L-CD40 interactions between $CD4^+$ Th cells and DCs (21) or $CD8^+$ T cells (25) also augment the generation of memory $CD8^+$ CTLs following virus (e.g., lymphocytic choriomeningitis virus [LCMV]) infection of mice (26–30). Simultaneous in vivo blockade of the CD28-CD80/86 and CD40-CD40L pathways, by coadministration of CTLA4Ig and anti-CD40L mAb, results in potent antigen-specific immunosuppression as evidenced by long-term acceptance of skin and cardiac allografts in mice (31) and renal allografts in rhesus macaques (32, 33).

In the current study, two groups of *Mamu A*01*$^+$ rhesus macaques (treatment or control, $n = 4$ per group) were infected with pathogenic SIVmac239. The treatment group received infusions of CTLA4-Ig and anti-CD40L mAb, which began 1 day prior to infection and continued for 27 days following SIV infection, according to a dose and schedule previously used to induce tolerance to MHC-mismatched renal allografts in rhesus macaques (see Methods). The use of *Mamu A*01*$^+$ macaques allowed us to track the development of SIV-specific $CD8^+$ T cell responses by flow-cytometric detection of $CD8^+$ T cells that bound tetrameric Mamu A*01 MHC complexes (tetramers) (34) that present known immunodominant $Gag_{181–189}$ (p11C, CTPYDINQM) and $Tat_{28–35}$ (SL8, STPESANL) SIV epitopes (35–37). To our knowledge this study represents the first use of CTLA4-Ig/anti-CD40L mAb-mediated CS blockade in primates wherein antigen-specific immune responses could be tracked longitudinally.

Methods

Animals and virus. Rhesus macaques (*Macacca mulatta*) used in this study harbored the *Mamu A*01* allele as determined through typing MHC class I alleles by PCR (38) (Supplemental Table 1; supplemental data available at http://www.jci.org/cgi/content/full/113/6/836/DC1). Male, 2.5- to 4.5-year-old, *Mamu A*01*$^+$ macaques were randomly assigned to treatment ($n = 4$) and control groups ($n = 4$). Recombinant human CTLA4-Ig and anti-CD40L (anti-gp39) mAb, which cross-reacts with macaque CD28 and CD40L (C. Larsen, unpublished results), were obtained from Bristol-Myers Squibb Co. (New York, New York, USA). Macaques in the CS blockade group received intravenous infusions of CTLA4-Ig (20 mg/kg) and anti-CD40L mAb (20 mg/kg) in sterile 0.9% sodium chloride solution (Baxter Healthcare Corp., Deerfield, Illinois, USA) 1 day prior to SIV infection and again on days 3, 6, 8, 10, 13, 20, and 27 following infection with SIV. Macaques in both CS blockade and untreated control groups were inoculated intravenously on day 0 with SIVmac239 (1.8 ng p27 per macaque; titered stock of SIVmac239 kindly provided by R. Desrosiers, Harvard Medical School, Boston, Massachusetts, USA) (39). Infected animals were maintained in accordance with institutionally and federally approved animal welfare protocols and standards.

Flow cytometry. Peripheral blood (heparinized) or lymph node cellular suspensions were stained for surface markers by incubation with titrated combinations of fluorochrome-conjugated Ab's obtained from BD Biosciences Pharmingen, San Diego, California, USA): FITC-, phycoerythrin–CD3ε (clone SP34), peridinin chlorophyll protein–CD8 (clone SK1), APC-CD4 (clone SK3), or APC-conjugated Mamu A*01 tetramers ($Gag_{181–189}$ and $Tat_{28–35}$). Contaminating red blood cells were lysed by incubation of samples with FACS Lysing Buffer (BD Biosciences Immunocytometry Systems, San Jose, California, USA). Intracellular staining with FITC-anti-Ki67 (clone B56; BD Biosciences Pharmingen) was performed following permeabilization of cells (FACS Permeabilizing Solution; BD Biosciences Immunocytometry Systems). Data were acquired (≥50,000 lymphocytes) on a FACSCalibur flow cytometer (BD Biosciences Immunocytometry Systems) and analyzed with FlowJo software (Treestar Inc., Ashland, Oregon, USA). For analyses, peripheral blood cells were gated on lymphocytes as determined by forward and side-scatter profiles. T cells were defined by positive staining with anti-CD3 Ab. For tetramer analyses, $CD8^+$ cells (medium and bright staining) that were identified within lymphocyte/$CD3^+$ gates were gated for binding to tetramer reagents and calculated as a percentage of $CD8^+$ T cells.

Enzyme-linked immunosorbent spot analysis of IFN-γ production. Multiscreen 96-well filter plates (Millipore, Billerica, Massachusetts, USA) were coated with anti–human-IFN-γ mAb (D1K; Biosource International, Camarillo, California, USA) in 0.1 M $NaHCO_3$ buffer (pH 9.5). Duplicate PBMC samples (500,000 per well) were stimulated in vitro with 2 μg/ml $Gag_{181–189}$ (p11C) peptide or negative control peptide (LCMV $NP_{396–404}$) in RPMI for 16–24 hours at 37°C, 5% CO_2. Bound IFN-γ was visualized following incubation of plates with biotinylated anti–human-IFN-γ mAb (7-B6-1; Mabtech AB, Nacka Strand, Sweden) and colorimetric detection by Vectastain ABC peroxidase kit (Vector Laboratories, Burlingame, California, USA) and stable 3,3′-diaminobenzidine (Research Genetics, Carlsbad, California, USA).

SIV viral load assay. Quantitative real-time RT-PCR assay to determine SIV viral load (40) was performed as described (41).

SIV sequence determination. Twenty thousand copies of viral RNA, determined by real-time RT-PCR quantification, were primed with random hexamers and reverse transcribed (Multiscribe RT) to produce cDNA. PCR amplification (40 cycles) of *tat* exon 1 was performed on 10,000 copy equivalents of cDNA per animal per time point with the following exceptions: day 42, Rvy5 = 8,000; day 42, Ryt5 = 7,250; day 42, RBm6 = 188 copy equivalents cDNA. PCR primers were as follows: SIV6511F (forward), 5′-AGTTAGCAAGCGAGGATCA-3′; SIV6900R (reverse), 5′-AGCAAGATGGCGATAAGCAG-3′ (9). PCR reaction products were gel purified and cloned into the pCR-BluntII-TOPO vector (Invitrogen Corp., Carlsbad, California, USA). Plasmid DNA was prepared using QIAprep Spin Minipreps (QIAGEN Inc., Valencia, California, USA) and used as the template for sequencing of insert DNA with M13 forward and M13 reverse primers. Automated DNA sequencing reactions were carried out by the Emory DNA Core Facility using fluorescent dye terminator cycle sequencing methodology. Sequence data were analyzed with Lasergene software suite (DNASTAR Inc., Madison, Wisconsin, USA).

Ab titers. Anti-SIV Ab titers were determined by Genetic Systems HIV-2 EIA (Bio-Rad Laboratories Virus Division, Redmond, Washington, USA) and expressed in arbitrary units that were derived from fitting A_{450} nm readings to the linear range of a standard curve that was generated from positive control (HIV-1) patient sera. Neutralizing Ab titers against SIVmac239 were measured as the reciprocal plasma dilution at which p27 production was reduced 80% in human PBMCs relative to the amount of p27 synthesized in the absence of a plasma sample (42). Neutralizing Ab titers against SIVmac251 were determined by CEMx174 cell-killing assay and are reported as the reciprocal plasma dilution at which 50% of cells were protected from virus-induced killing as measured by neutral red uptake (42).

Statistics. Repeated measures analyses (43) for each outcome were performed using a means model (SAS PROC MIXED) with

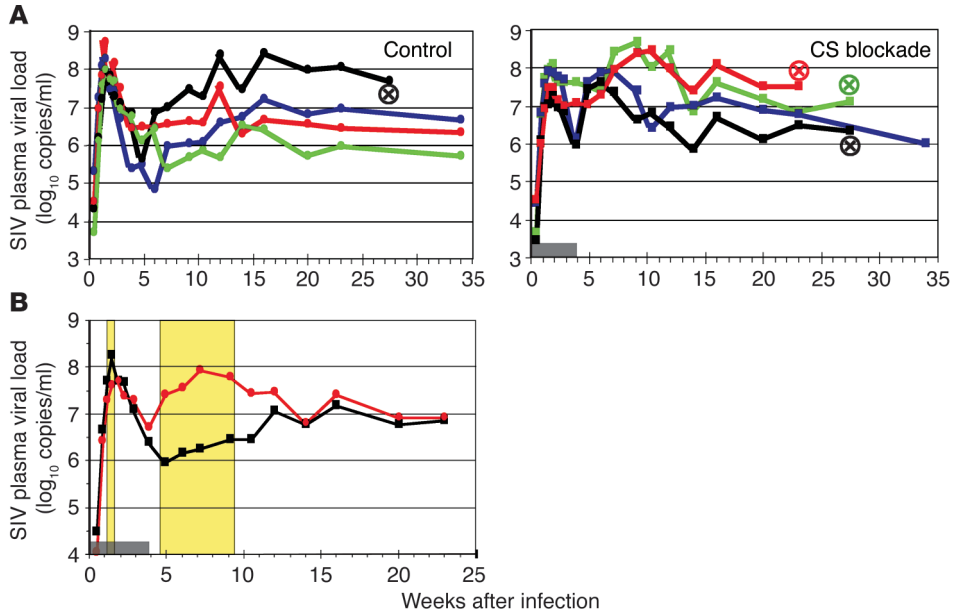

Figure 1
Effects of CS blockade on SIV replication. (**A**) SIV viral load (log_{10} SIV RNA copies per milliliter plasma) from macaques in the control group (left panel) or CS blockade treatment group (right panel). Indicated are times at which individual macaques were sacrificed because of clinical deterioration due to simian AIDS (circled x). Control macaques: ROz5 (black), RBm6 (blue), RVy5 (red), RYt5 (green). CS blockade macaques: REp6 (black), REo6 (blue), RIc6 (red), RCr5 (green). The gray bar denotes the treatment period. (**B**) Geometric mean SIV viral load (log_{10} SIV RNA copies per milliliter plasma) for CS blockade group (red) and control group (black). The yellow shading indicates times at which significant differences were determined between groups ($P \leq 0.05$, repeated measures analysis of means). The gray bar denotes the treatment period.

SAS/STAT (SAS Institute, Cary, North Carolina, USA), providing separate estimates of the means by days after infection and treatment group. A compound symmetry variance-covariance form among the repeated measurements was assumed for each outcome, and robust estimates of the standard errors were used to perform tests and construct 95% confidence intervals. Fisher's exact, Mann-Whitney, Spearman correlation, and *t* tests were calculated with the StatView software package (SAS Institute).

Results

Effects of CS blockade on SIV replication. We first determined the effects of transient T cell CS blockade on SIVmac239 replication by measuring levels of SIV in plasma by a quantitative real-time RT-PCR assay (Figure 1). Macaques in both treatment and control groups exhibited similar rates of initial increase in SIV viremia ($P = 0.82$, comparison of regression slopes between groups, days 3–10 after infection; Figure 1A). Peak SIV viremia in the control group (day 10, log_{10} geometric mean viral RNA (vRNA) = 8.26) occurred earlier (at day 10 after infection in three of four macaques) than in the treatment group (at day 13 after infection in four of four macaques) and was significantly greater (fourfold) than the corresponding level of viremia in the treatment group (day 10 log_{10} vRNA = 7.62; $P = 0.009$, repeated measures analysis of means; Figure 1B, shaded region). Comparison of postpeak declines in SIV viremia (through day 27 after infection, the last day of treatment) revealed that untreated control macaques exhibited an average 1.86 log reduction in viral load (range = 1.08–2.88), whereas treated animals exhibited a 1 log reduction in postpeak SIV viremia (range = 0.46–1.74). Control macaques (three of four) exhibited continued declines in SIV viremia for an additional 1–2 weeks. Following cessation of CTLA4-Ig and anti-CD40L mAb infusions, treated macaques displayed a transiently (approximately 4 weeks) increased geometric mean level of SIV viremia that was significantly greater (21- to 30-fold) than that observed in control animals (Figure 1B, shaded region). During the same period of time, the control group exhibited a gradual progressive increase (threefold) in geometric mean SIV viral load (Figure 1B). By 14 weeks after infection, both groups reached similar set point levels of SIV plasma viremia at approximately 10^7 SIV RNA copies per milliliter (Figure 1B). Thus, CS blockade during acute SIV infection had a moderate, but significant effect on the level and timing of peak SIV viremia and reduced control (in both magnitude and duration) of postpeak viral load, but did not affect ultimate set point levels of SIV viremia.

CS blockade attenuates SIV-specific CD8⁺ T cell responses. Macaques undergoing CS blockade generated substantially reduced levels of SIV $Gag_{181–189}$- and $Tat_{28–35}$-specific $CD8^+$ T cells compared with untreated control animals during acute SIV infection (Figure 2A). In control macaques, $CD8^+$ T cells directed against the $Gag_{181–189}$ epitope were detected in peripheral blood as early as 10 days following SIV infection (Figure 2A) and exhibited a mean peak level of 2.6% (range = 2.3–3.2%) at day 13 after infection. In contrast, macaques in the treatment group exhibited a significantly lower (eightfold) mean level of $Gag_{181–189}$-specific $CD8^+$ T cells (0.34%, range = 0.21–0.43%; $P < 0.0001$, *t* test). In treated macaques, the mean peak level of $Tat_{28–35}$-specific $CD8^+$ T cells was reduced and occurred earlier than in control macaques (CS peak day 16, mean = 1.1%, range = 0.7–2.0%; control peak, day 20, mean = 3.2%, range = 1.3–8.2%; $P = 0.04$ Mann-Whitney *U* test) (Figure 2A).

Measurement of $CD8^+$ T cells directed against only two Mamu A*01–restricted SIV epitopes ($Gag_{181–189}$ and $Tat_{28–35}$) assesses only a subset of the total potential $CD8^+$ T cell responses mounted by individual outbred macaques against SIV (36). We reasoned that measurement of in vivo $CD8^+$ T cell proliferation during acute SIV infection may predominantly reflect antigen-specific expansion of SIV-specific precursors, rather than nonspecific $CD8^+$ T cell activation or homeostatic lymphocyte proliferation. This is because initial increases in the levels of proliferating $CD8^+$ T cells coincides temporally with the emergence of SIV-specific $CD8^+$ T cell responses of known epitope specificities (Figure 2, A and B) and because the acute $CD8^+$ T cell proliferation that occurs in other experimental viral infections predominantly reflects viral antigen-specific responses (44). We measured acute $CD8^+$ T cell proliferation in SIV-infected macaques by flow-cytometric detection of the Ki67 (45), a nuclear antigen that identifies cells progressing through the cell cycle (i.e.,

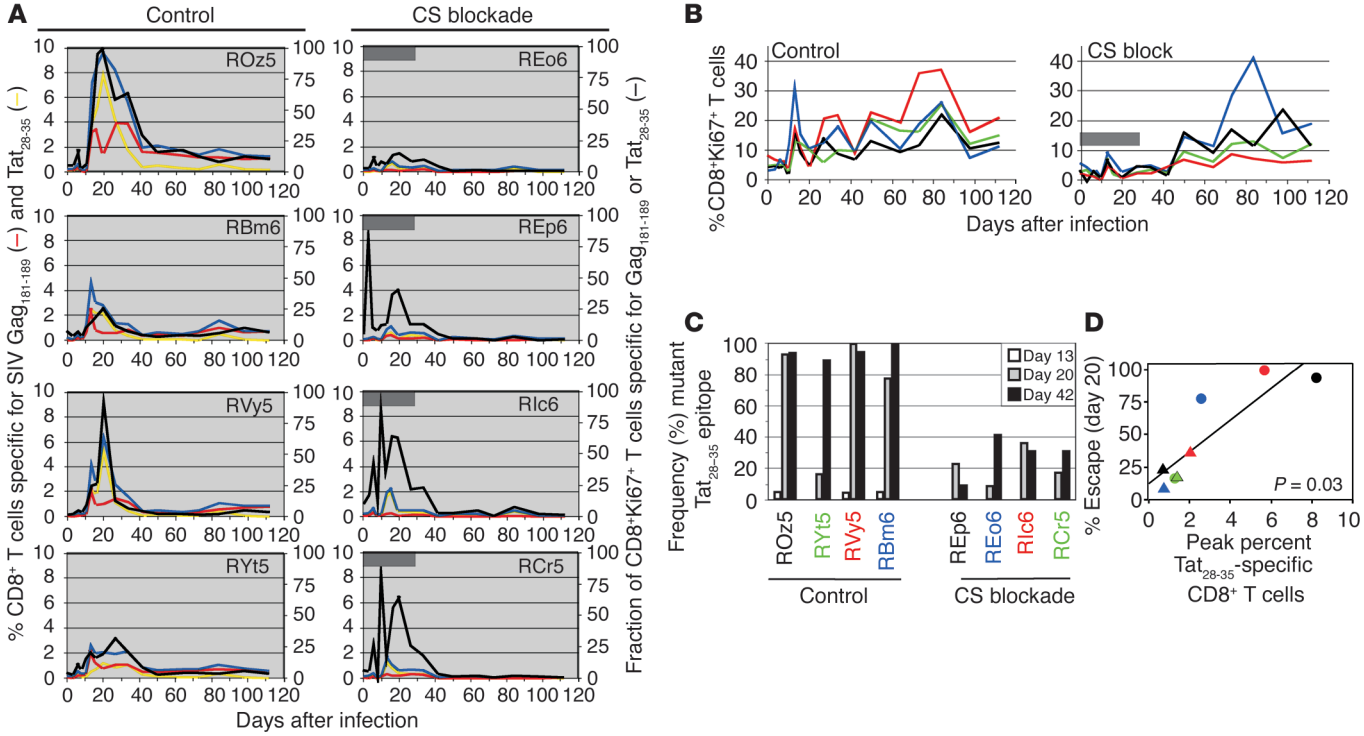

Figure 2

CS blockade attenuates the generation and in vivo CTL activity of SIV-specific CD8+ T cell responses. (**A**) Levels of $Gag_{181–189}$-specific (CTPYDINQM-specific) CD8+ T cells (red trace), $Tat_{28–35}$-specific (STPESANL-specific) CD8+ T cells (yellow trace), or the sum of $Gag_{181–189}$- and $Tat_{28–35}$-specific CD8+ T cells (blue trace) as percentages of CD8+ T cells in peripheral blood (left axes) and the level of the sum of $Gag_{181–189}$- and $Tat_{28–35}$-specific CD8+ T cells as a percentage of CD8+Ki67+ T cells (black trace) in peripheral blood (right axes). Left column, control macaques; right column, CS blockade macaques. Gray bars denote the treatment period. (**B**) Levels (%) of peripheral blood CD8+ T cells that exhibit the Ki67 antigen, a marker of cellular proliferation, by flow cytometry. Control macaques: ROz5 (black), RBm6 (blue), RVy5 (red), RYt5 (green). CS blockade macaques: REp6 (black), REo6 (blue), RIc6 (red), RCr5 (green). The gray bar denotes the treatment period. (**C**) Nucleotide sequences of cDNA clones encoding SIV *tat* exon 1 were determined at the indicated times after infection and were compared to the WT parental SIVmac239 sequence. Frequencies of cDNA clones that exhibited one or more nonsynonymous mutations within the region encoding the $Tat_{28–35}$ (STPESANL) epitope are shown for individual macaques in the control or CS blockade groups. (**D**) Correlation of the level of $Tat_{28–35}$-specific (STPESANL-specific) CD8+ T cells and the frequency of mutation within the $Tat_{28–35}$ coding region at 20 days following SIV infection. The *P* value was determined by the Spearman rank correlation test. Control macaques (circles): ROz5 (black), RBm6 (blue), RVy5 (red), RYt5 (green); CS blockade macaques (triangles): REp6 (black), REo6 (blue), RIc6 (red), RCr5 (green).

not in G_0) (46, 47). Untreated macaques exhibited a significant increase (fourfold) over baseline in the mean level of proliferating CD8+ T cells (day 13 after infection, $P = 0.02$, *t* test) that coincided temporally with the peak $Gag_{181–189}$-specific CD8+ T cell response. In contrast, this acute CD8+ T cell proliferative response was blunted in macaques undergoing CS blockade (twofold increase over baseline at day 13 after infection) (Figure 2B). The fraction of proliferating CD8+ T cells that were specific for $Gag_{181–189}$ or $Tat_{28–35}$ was calculated to assess the focus of each macaque's anti-SIV CD8+ T cell response to these previously defined $Gag_{181–189}$ and $Tat_{28–35}$ Mamu A*01–restricted epitopes (Figure 2A, black traces). Because this parameter is calculated from independent measurements of CD8+Ki67+ and CD8+ tetramer-positive lymphocytes, it potentially reflects a partial contribution from changes in CD8+ T cell homeostatic proliferation or aberrant cell cycle arrest. At the times of peak responses, $Gag_{181–189}$- and $Tat_{28–35}$-specific CD8+ T cells accounted for 20–100% of the CD8+ T cell proliferative response in control animals and 15–100% in treated macaques. The relatively narrow antigenic focus of CD8+ T cell responses exhibited during acute SIV infection of some macaques may be due to homozygosity of the *Mamu A*01* allele (e.g., ROz5 typed positive only for the *Mamu A*01* MHC allele out of eight different MHC-I alleles assayed; see Supplemental Table 1) or to exceptional immunodominance of Mamu A*01–restricted $Gag_{181–189}$ and $Tat_{28–35}$ epitopes over others potentially restricted by additional (but unidentified) MHC class I alleles.

CS blockade attenuates in vivo SIV-specific CTL function. To assess CD8+ CTL effectiveness in vivo, frequencies of SIV $Tat_{28–35}$ CTL escape mutants (9) were determined at 13, 20, and 42 days following SIV infection of macaques (Figure 2C; see also Supplemental Table 2). Frequencies of CTL-escape mutants were determined as the number of SIV cDNA clones that harbored one or more nonsynonymous mutation within the region encoding the $Tat_{28–35}$ epitope per total cDNA clones analyzed. Nonsynonymous mutations in *tat* exon 1, when present, occurred almost exclusively within the region encoding the $Tat_{28–35}$ epitope (representative alignments shown in Supplemental Figure 1).

Treated macaques, which exhibited lower levels and shorter duration of $Tat_{28–35}$-specific CD8+ T cells than untreated controls (Figure 2A), also harbored significantly lower frequencies of $Tat_{28–35}$ CTL-escape mutants (Figure 2C). At day 13 after infection, mutation within the region encoding the $Tat_{28–35}$ epitope was observed only in cDNA clones from control macaques (≤5%) (Figure 2C). At 20 days

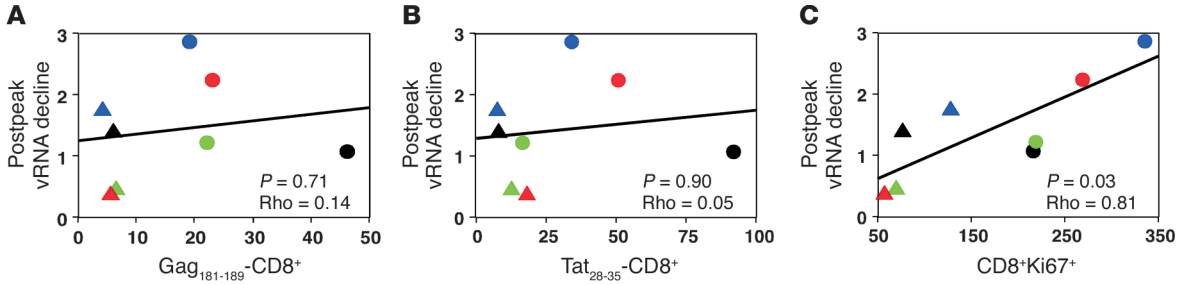

Figure 3

Reduction of acute SIV viral load is directly related to CD8+ T cell proliferative responses. Correlation of the magnitude of postpeak decline in SIV viremia and $Gag_{181–189}$-specific (**A**), $Tat_{28–35}$-specific (**B**), and Ki67+ (**C**) CD8+ T cells. The magnitude of the postpeak decline in SIV viremia is reported as the logarithm of the fold reduction of SIV viremia between peak and day 27 after infection (last day of treatment). All CD8+ T cell parameters were calculated as AUCs from baseline through day 27 after infection. Control macaques (circles): ROz5 (black), RBm6 (blue), RVy5 (red), RYt5 (green); CS blockade macaques (triangles): REp6 (black), REo6 (blue), RIc6 (red), RCr5 (green). *P* and ρ values were determined by the Spearman rank correlation test. The solid lines are regression lines.

after infection, the time point that corresponded with the peak $Tat_{28–35}$-CD8+ T cell response in this group, three of four control macaques exhibited mutation frequencies greater than 77% (Figure 2C). The fourth control animal, Ryt5, exhibited a lower frequency of mutation at day 20 after infection (17% mutant clones) and also exhibited the lowest peak level of $Tat_{28–35}$-specific CD8+ T cells among animals in the control group (Figure 2, A and C). Treated animals exhibited significantly lower frequencies of mutation within the $Tat_{28–35}$ epitope at days 20 and 42 following infection as compared with controls (CS block versus control: day 20, $P < 0.0001$; day 42, $P < 0.0001$; Fisher's exact test). Identical results were obtained when these analyses were performed using a restricted definition of an escape mutant as one that had previously been shown to exhibit impaired binding to the Mamu A*01 MHC-I molecule (Table 1 in ref. 9). Overall, a significant positive correlation ($P = 0.028$, $\rho = 0.83$, Spearman rank correlation) was observed between the peak level of $Tat_{28–35}$-specific (STPESANL-specific) CD8+ T cells (observed during the first 20 days following SIV infection) and the frequency of SIV sequence clones (at 20 days after infection) that harbored one or more nonsynonymous mutations within the region encoding the $Tat_{28–35}$ epitope (Figure 2D). These results provide strong evidence for in vivo CD8+ T cell–mediated selection against the WT $Tat_{28–35}$ (STPESANL) epitope and ensuing virus escape from $Tat_{28–35}$-specific CD8+ T cells by mutation (9, 48). Furthermore, because $Tat_{28–35}$-specific CD8+ T cells became undetectable following acute infection of treated macaques (Figure 2A), even though WT SIV still predominated (Figure 2C), these results demonstrate that emerging antiviral CD8+ T cell function is abrogated in the setting of CS blockade.

Acute SIV viral load is inversely related to acute CD8+ T cell proliferative responses. The correlation of acute $Gag_{181–189}$- and $Tat_{28–35}$-specific CD8+ T cell responses with postpeak reduction in SIV viral load revealed only weak trends that did not achieve statistical significance (Figure 3, A and B). The SIV-specific CD8+ T cell responses mounted by our cohort of outbred animals, as measured by the available MHC class I tetramers, may not reflect total SIV-specific CD8+ T cell responses, as suggested by the observation that they represent only a fraction of CD8+Ki67+ T cells. Therefore, we also considered acute (through day 27 after infection) levels of total CD8+ T cell proliferation (CD8+Ki67+ T cells) as a surrogate measure of SIV-specific CD8+ T cell responses directed against all existing and newly emerging SIV epitopes (44). Using this measure, it was found that in vivo CD8+ T cell proliferation during acute SIV infection was significantly correlated with the magnitude of postpeak decline in SIV viremia ($P = 0.03$, Figure 3C). Similarly, a more sensitive mathematical modeling analysis of our data that takes into account all available information on target cells and SIV-specific CD8+ T cells during primary infection shows that SIV-specific CD8+ T cell responses play a crucial role in the control of early SIV replication in the untreated macaques, whereas SIV replication kinetics in macaques undergoing CS blockade are the result of target cell exhaustion (49).

Chronic SIV-specific CD8+ T cell responses are impaired following acute CS blockade. In the absence of effective CS, T cells exposed to antigen can become anergic or undergo apoptosis (50). Similarly, in the absence of effective CD4+ T cell help during chronic viral infection, viral antigen-specific CD8+ T cells may also become anergic or undergo deletion (51). The relatively shorter duration and lower levels, of $Gag_{181–189}$- or $Tat_{28–35}$-specific CD8+ T cells observed in treated

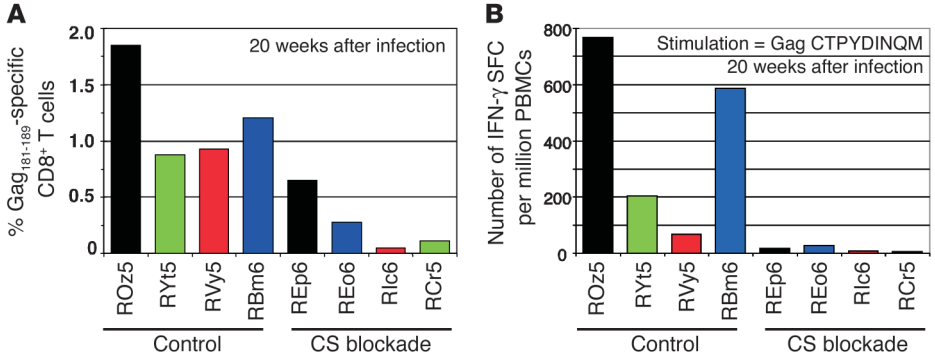

Figure 4

Chronic SIV-specific CD8+ T cell responses are impaired following acute CS blockade. Levels of $Gag_{181–189}$-specific (CTPYDINQM-specific) CD8+ T cells determined by tetramer staining of peripheral blood at 20 weeks following SIV infection (**A**) and corresponding ELISPOT quantification of IFN-γ–producing cells following in vitro stimulation of PBMCs with $Gag_{181–189}$ (CTPYDINQM) peptide (**B**).

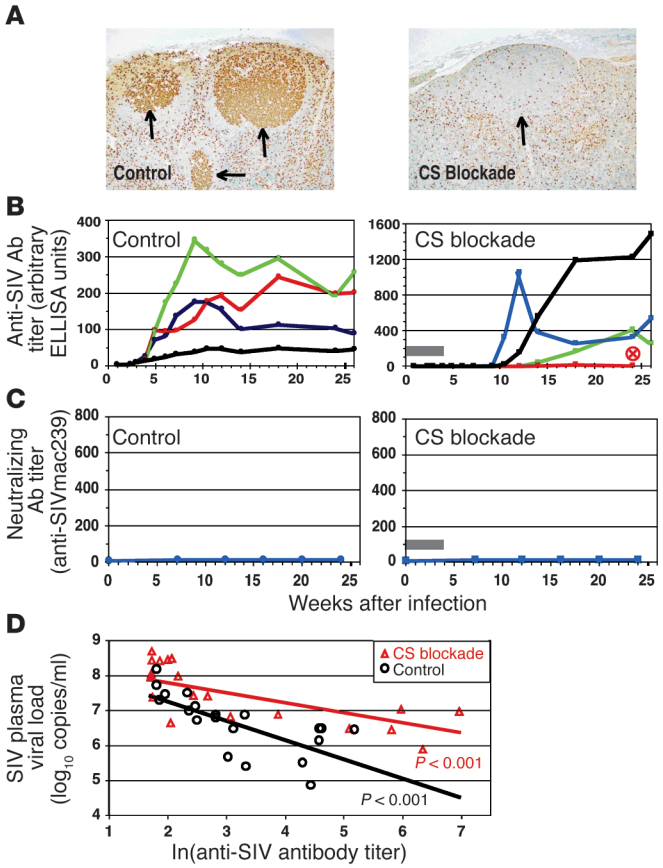

Figure 5

Effects of acute CS blockade on humoral immune responses. (**A**) B cell germinal centers (arrows) in representative lymph node sections from macaques in control or treatment (CS blockade) groups at 10 days following SIV infection. Ki67$^+$ lymphocytes are brown; magnification ×200. (**B** and **C**) SIV-specific Ab titers were determined by ELISA (**B**) or SIVmac239-neutralization assay (**C**) on plasma samples from control macaques (circles): ROz5 (black), RBm6 (blue), Rvy5 (red), RYt5 (green); or CS blockade macaques (triangles): REp6 (black), REo6 (blue), RIc6 (red), RCr5 (green). Gray bars denote the treatment period; note different scales. (**D**) Correlation of SIV-specific Ab titer (by ELISA) and SIV plasma viral load around the time of seroconversion for macaques in the control group (days 16–42 after infection) or CS blockade–treatment group (days 50–98 after infection). Ab titers are plotted as natural log transforms of the Ab titers in **B**.

macaques is consistent with this model (Figure 2A). Interestingly, $Gag_{181–189}$-specific CD8$^+$ T cells were detected by tetramer staining in treated animals beginning at 18 weeks after infection (14 weeks following cessation of the CS blockade, data not shown). The $Gag_{181–189}$-specific CD8$^+$ T cells that emerged during chronic infection of treated macaques may represent new thymic emigrants that are (partially) responsive to high levels of SIV antigen. Alternatively, these cells may have arisen from CD8$^+$ $Gag_{181–189}$-precursors within the naive repertoire, which were present at initial SIV infection, but whose expansion was blocked during the period of effective CS blockade. We performed enzyme-linked immunosorbent spot (ELISPOT) assays to assess the functional capacity of SIV-specific CD8$^+$ T cells. The $Gag_{181–189}$-specific CD8$^+$ T cells that emerged late (20 weeks after infection) in (two of four) treated animals (Figure 4A) exhibited attenuated production of IFN-γ in response to in vitro stimulation with cognate $Gag_{181–189}$ (CTPYDINQM) peptide (Figure 4B). This impairment of SIV-specific CD8$^+$ T cells that arose during chronic SIV infection is consistent with functional exhaustion or impaired induction of CD8$^+$ T cell responses that are generated in the absence of effective CD4$^+$ T cell help (51–53).

Acute CS blockade delays SIV seroconversion. We characterized the development of humoral immune responses against SIV in treated versus control macaques and determined their relationship to SIV replication. Development of B cell germinal centers (GCs) in lymph nodes, assessed by histological analysis of proliferating (Ki67$^+$) lymphocytes, was evident at 10 days following SIV infection of control macaques but was profoundly inhibited in treated animals (Figure 5A). Similar inhibition of GC development by CS blockade was also observed in lymph nodes from treated animals at 6 weeks after infection (not shown) and is temporally consistent with the delayed seroconversion observed in treated animals (Figure 5B). These effects on GC development and seroconversion are consistent with the inhibitory effects on humoral immunity following in vivo disruption of CD40L-CD40 lymphocyte signaling in other animal models (24).

While animals in both control and treatment groups exhibited seroconversion against SIV, albeit with different kinetics, in neither group did macaques produce Ab's that were able to neutralize SIVmac239 infection ex vivo (Figure 5C). Interestingly, SIV-specific Ab's that were elicited during SIVmac239 infection of both treated and control macaques, while not capable of neutralizing SIVmac239, were capable of ex vivo neutralization of a related tissue culture–adapted SIV isolate (SIVmac251) (Supplemental Figure 2). The delayed emergence of SIVmac251-specific neutralizing Ab's in treated versus control macaques (Supplemental Figure 2) indicates that generation of neutralizing Ab responses against SIV is prevented by the CS blockade. These Ab responses therefore must require effective CD4$^+$ T cell help and do not arise in a T cell–independent manner, as previously suggested (42, 54).

SIV viral load is inversely related to SIV-specific Ab titers. In both groups, significant inverse correlations were observed between the levels of SIV plasma viremia and SIV-specific Ab titers around their respective times of seroconversion (Figure 5D; control group, $P < 0.001$; CS blockade group, $P < 0.001$: comparison of slopes of regression lines against zero; that is, null hypothesis indicates no association). This inverse correlation was greater for the control group than for the treatment group (Figure 5D; $P = 0.03$, comparison of slopes for control versus treatment group). In addition, inverse rank order correlations between SIV plasma viremia and SIV-specific Ab titers were observed in individual animals at numerous time points following seroconversion that extend into the period of steady-state SIV viremia (compare Figure 1A and Figure 5B).

Peak SIV viremia is predicted by early levels of proliferating CD4$^+$ T cells. Upon infection with a CD4$^+$-tropic lentivirus, activated virus-specific CD4$^+$ T cells can act as both targets for productive viral infection and as effector Th cells that augment antiviral humoral and cellular immune responses. Because SIV replication is augmented in activated/proliferating CD4$^+$ T cells (versus resting cells) both in vitro (55) and in vivo (56), we reasoned that levels of in vivo proliferating target cells that precede the development of antiviral effectors should predict the ensuing peak of SIV viremia. At 10 days following SIV infection, the level of proliferating CD4$^+$ T cells (CD4$^+$Ki67$^+$) in lymph nodes, an anatomic site that supports high levels of SIV replication (57), exhibited a significant direct correlation with peak SIV plasma viremia (Figure 6A; $P = 0.03$, Spearman's $\rho = 0.81$). Similarly, a significant direct correlation was also observed

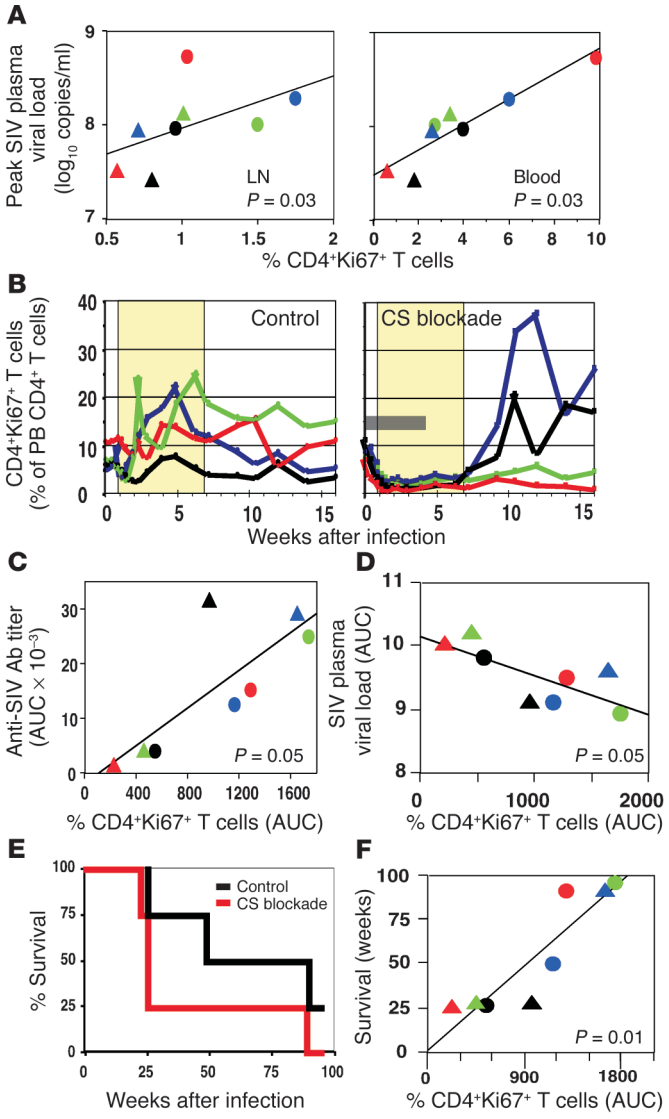

Figure 6
In vivo CD4+ T cell proliferative responses predict the peak level and subsequent control of SIV viremia, titers of SIV-specific Ab's, and survival of infected macaques. (**A**) Correlation between the level of CD4+Ki67+ T cells (day 10 after infection) in lymph node or peripheral blood and peak SIV plasma viremia. (**B**) Levels of CD4+Ki67+ T cells in peripheral blood of macaques in the control group and treatment group (CS blockade). The yellow shading indicates times at which significant differences were determined between groups ($P = 0.05$, repeated measures analysis of means). The gray bar denotes the treatment period. (**C** and **D**) Correlation between the level of CD4+Ki67+ T cells in peripheral blood (AUC: baseline to 16 weeks after infection) and level of anti-SIV Ab's (AUC: day 6–18 weeks after infection) (**C**) or the level of SIV plasma viremia (AUC: day 3–16 weeks after infection) (**D**). (**E**) Survival of macaques in the control (black) or CS blockade treatment group (red). (**F**) Correlation between CD4+Ki67+ T cells (AUC: baseline to 16 weeks after infection) and period of survival. (**A**, **C**, **D**, and **F**) Treated macaques, triangles; control macaques, circles. *P* values were determined by the Spearman rank correlation test. The solid lines represent regression lines. (**A**, **B**, **C**, **D**, and **F**) Control macaques: ROz5 (black), RBm6 (blue), RVy5 (red), RYt5 (green); CS blockade macaques: REp6 (black), REo6 (blue), RIc6 (red), RCr5 (green). PB, peripheral blood.

between the level of proliferating CD4+ T cells (CD4+Ki67+) in peripheral blood (day 10 after infection) and peak SIV viremia (Figure 6A; $P = 0.02$, Spearman's $\rho = 0.90$). These data provide direct evidence that higher levels of activated CD4+ T cells in vivo during the initial phase of SIV infection contribute to increased levels of SIV viremia. The fact that control macaques exhibited higher levels of CD4+ T cell proliferation in lymph nodes and blood (Figure 6A; lymph nodes, $P = 0.04$; blood, $P = 0.04$; Mann-Whitney *U* test) than did macaques undergoing CS blockade indicates that this increased CD4+Ki67+ response in control animals reflects antigen-driven proliferation of SIV-specific CD4+ T cells.

SIV viral load is inversely related to CD4+ T cell proliferative responses. SIV-infected CD4+ T cells, including those specific for SIV as well as other antigens, serve as a source of SIV production during infection. Additionally, SIV-specific CD4+ T cells also potentially function as antiviral effectors through direct and/or indirect mechanisms. To examine the relationship between CD4+ T cell responses to SIV infection and viral load, we measured in vivo CD4+ T cell proliferation during the first four months of SIV infection (Figure 6B) and compared this with SIV-specific Ab responses (Figure 6C) and viral loads (Figure 6D). Acute CS blockade treatment of SIV-infected macaques resulted in a significant reduction in levels of proliferating (Ki67+) CD4+ T cells in peripheral blood as compared with untreated control animals (Figure 6B). The mean level of CD4+Ki67+ T cells in treated macaques, which decreased threefold below baseline level during the first week of treatment, did not increase during acute SIV infection as was observed for untreated controls, and remained suppressed through at least 7 weeks after infection (Figure 6B). This observation is most readily explained by destruction of highly permissive (Ki67+) CD4+ T cells by SIV infection and the simultaneous prevention of expansion of SIV-specific CD4+ T cells by effective CS blockade.

Following cessation of the CS blockade, delayed recovery of CD4+ T cell proliferation was observed in two of four treated macaques, and this CD4+ T cell response correlated temporally with SIV seroconversion (Figure 5B and Figure 6B). For treated and control macaques, the duration and magnitude of CD4+Ki67+ T cell responses measured in peripheral blood during the initial 4 months of SIV infection, measured as area under the curve (AUC) (Figure 6B) correlated significantly with the cumulative SIV-specific Ab response (AUC, Figure 5B) ($P = 0.05$, Spearman rank correlation; Figure 6C). Moreover, comparison of AUCs for SIV viremia and CD4+Ki67+ T cell levels, as measures of their magnitude and duration, also revealed a significant correlation between in vivo CD4+ T cell proliferation and lower SIV plasma viral load (Figure 6D; $P = 0.05$, Spearman rank correlation). In contrast, similar analyses did not reveal any significant associations between CD8+ T cell proliferation and SIV viral load (Supplemental Figure 3).

In vivo CD4+ T cell proliferative responses predict survival. Because in vivo levels of CD4+Ki67+ T cells correlated with increased anti-SIV humoral immunity and decreased SIV viremia, we reasoned that the in vivo CD4+ T cell proliferative response to infection, if protective, should also correlate with increased periods of survival of infected macaques. Within the treatment group, three of four macaques progressed rapidly to simian AIDS (≤25 weeks post-infection), whereas only one of four control macaques exhibited accelerated disease progression (Figure 6E). The magnitude and duration of CD4+ T cell proliferation (measured as AUC; Figure 6B) exhibited a significant direct correlation with increased periods of survival for macaques in both the treatment and control groups (Figure 6F; $P = 0.01$, Spear-

man's $\rho = 0.952$), whereas absolute levels of peripheral blood $CD4^+$ T cells (which were similar between treatment and control groups) were not associated with survival (Supplemental Figure 4).

Discussion

The relative roles played by multiple host immune responses in regulating HIV replication and the mechanisms underlying their ultimate failure to successfully control virus infection and prevent immunodeficiency disease progression remain incompletely understood. For a better understanding of the relative contributions of antiviral $CD8^+$ T cells, $CD4^+$ target cells, antiviral $CD4^+$ Th cells, and Ab responses in modulating $CD4^+$-tropic lentivirus replication and pathogenesis, we have used CTLA4-Ig/anti-CD40L mAb-mediated blockade of in vivo T cell CS pathways during acute SIV infection of rhesus macaques. We show here that transient in vivo CS blockade during acute SIV infection of rhesus macaques results in attenuation of SIV-specific cellular and humoral immune responses and a reduced capacity to control acute SIV replication. We conclude that control of postpeak viremia during acute (untreated) SIV infection is largely mediated by SIV-specific $CD8^+$ T cells, which is in agreement with previous studies predicated on mAb-mediated depletion of CD8α-expressing cells (12–14). This conclusion is supported by correlational analyses presented here (Figure 3), as well as by our results from mathematical modeling of this data set to discriminate between target cell limitation versus immune control models of acute SIV replication (49).

We found evidence for $CD8^+$ T cell–mediated control of SIV replication at early, but not late, times following infection. Interestingly, the magnitude of decline in postpeak SIV viremia correlates more strongly with the acute $CD8^+$ T cell proliferative response to SIV infection, a surrogate measure of total SIV-specific $CD8^+$ T cell responses, than with either of two specific immunodominant $CD8^+$ T cell responses ($Gag_{181–189}$ and $Tat_{28–35}$) and suggests that the predominance of these Mamu-A*01–restricted $CD8^+$ T cell responses does not necessarily imply effective control of SIV replication. While our studies do not indicate the precise mechanism through which $Gag_{181–189}$-specific $CD8^+$ T cells fail to contain SIV replication, it is conceivable that multiple mechanisms, including SIV escape from CTL recognition by epitope mutation (9, 10), as shown for the $Tat_{28–35}$ epitope STPESANL (Figure 2D), improper differentiation in the setting of chronic antigen exposure (58, 59), dysregulation of CTL effector mechanisms (58, 60–62), and inefficient killing of infected targets by CTL (63), may function simultaneously to render particular SIV-specific $CD8^+$ T cell responses ineffective at controlling SIV replication.

In addition to the role of $CD8^+$ T cells in regulation of acute SIV replication, our results highlight the dual role of SIV-specific $CD4^+$ T cells as both targets for productive virus infection and antiviral Th cells. At the earliest stages of SIV infection, activated/proliferating $CD4^+$ T cells (of all antigenic specificities) that become infected appear to contribute to net increases in SIV viremia. Subsequent expansion of virus-specific $CD4^+$ T cells, which, by analogy to HIV infection, may be preferentially infected with SIV (64), in turn may lead to either further increases in SIV viremia by providing an expanded pool of permissive target cells or lead to a decline in SIV viremia through exertion of antiviral effects. Our finding that duration and levels of proliferating $CD4^+$ T cells in circulation are directly correlated with titers of SIV-specific Ab's and indirectly correlated with SIV viremia provides strong, albeit indirect, evidence that the observed in vivo $CD4^+$ T cell proliferative response is composed largely of SIV-specific $CD4^+$ T cells that are responding to SIV as an antigen and may, to various degrees, exert a net antiviral effect. The alternative scenario, as envisioned in "tap and drain" models of HIV pathogenesis (65), is that $CD4^+$ T cell proliferation occurs as a compensatory response to an imbalance in lymphocyte homeostasis caused by increased destruction of $CD4^+$ T cell targets. This model, which predicts a direct correlation between levels of $CD4^+$ T cell proliferation and SIV viremia, does not appear likely in light of our data.

Our observation, in both treated and untreated macaques, that increased titers of nonneutralizing SIV-specific Ab's are associated with lower SIV viral loads at their respective times of seroconversion suggests that production of these Ab's constitutes one potential mechanism of antiviral regulation, but does not exclude additional potential mechanisms, such as production of antiviral cytokines and chemokines by underlying SIV-specific $CD4^+$ Th cell responses. Nonneutralizing SIV-specific Ab's potentially function to lower levels of SIV replication through Ab-dependent cellular cytoxicity–mediated clearance of infected cells (66) and by clearance, via the mononuclear phagocytic system, of virions in complement-containing immune complexes (67). Because SIVmac239 is less susceptible to Ab-mediated neutralization than are other SIV strains (e.g., SIVmac251), our use of SIVmac239 in this study likely underestimates the potential antiviral effects of neutralizing Ab's (68). Moreover, the observation that SIV seroconversion and concomitant reduction in SIV viral load occurred prior to the emergence of SIV-specific ($Gag_{181–189}$-specific) $CD8^+$ T cells in treated macaques further suggests that SIV-specific Ab's (or another aspect of the underlying SIV-specific $CD4^+$ T cell response) mediate reduction of SIV viremia, independent of $CD4^+$ Th effects on $CD8^+$ CTLs. Regardless, the observations that, over time, an increased $CD4^+$ T cell proliferative response to SIV infection predicts increased titers of SIV-specific Ab's, lower viral load, and increased time of survival provide evidence that this response is composed of SIV-specific $CD4^+$ T cells that exert an antiviral effect.

Progressive loss of peripheral $CD4^+$ T cells in association with progressive susceptibility to opportunistic infections, a hallmark of HIV infection that occurs by accelerated destruction and impaired regeneration of this cell population (reviewed in ref. 69), was also observed in SIV-infected macaques with increasing duration of SIV infection. The end-stage levels of peripheral blood $CD4^+$ T cells, however, did not correlate with time of AIDS-free survival (Supplemental Figure 4). In light of these results, progression to simian AIDS that follows infection with highly virulent isolates of SIV (such as SIVmac239), as evidenced by severe weight loss and development of multiple opportunistic infections, likely reflects a pronounced impairment of $CD4^+$ T cell functionality in addition to actual depletion of peripheral blood $CD4^+$ T cells. In this regard, the use of such virulent SIV isolates may mask subtleties relevant to understanding HIV pathogenesis in humans. During HIV infection of humans, reduced numbers of peripheral blood $CD4^+$ T cells have been shown to correspond with an increased fraction of proliferating cells within this compartment (70). Because the extent of depletion of peripheral blood $CD4^+$ T cells in humans with progressive HIV infection appears to be greater than that occurring in SIV-infected macaques (71), coincident increases in fractions of proliferating $CD4^+$ T cells in humans may exhibit a positive association with disease progression, whereas the magnitude and duration of the in vivo $CD4^+$ T cell proliferative response during SIV infection of macaques is predictive of increased periods of AIDS-free survival.

In this regard, it is becoming increasingly appreciated that the deleterious "indirect" consequences of chronic, generalized immune activation, in addition to direct virus-mediated killing of $CD4^+$ T cells, play prominent roles in the pathogenesis of AIDS

(72–75). Important evidence supporting the view that generalized immune activation is a primary determinant of disease progression following CD4-tropic lentivirus infection of humans and nonhuman primates that are not natural hosts of these viruses (such as rhesus macaques) is the observation that apathogenic SIV infection of natural host species, such as sooty mangabey monkeys, is characterized by limited bystander immunopathology despite chronic high-level SIV viremia (74). Given that experimental SIV infection of rhesus macaques leads to high levels of immune activation and progression to AIDS, it is conceivable that CS blockade in SIV-infected rhesus macaques might have resulted in attenuation, rather than aggravation, of disease progression through reduction of the pathogenic role of immune activation. This outcome, however, was clearly not observed, potentially the result of a number of factors. First, transient administration of CS blockade reagents in rhesus macaques did not induce either complete or durable tolerance against SIV antigens, as revealed through longitudinal assessments of SIV antigen-specific immune responses (Figure 4A and Figure 5B). This impermanent attenuation of immune responses by CS blockade in macaques is in contrast to the more pronounced and durable effects of transient CS blockade in induction of antigen-specific immune tolerance in mice (31). Second, the control of immunopathology in SIV-infected sooty mangabey monkeys might be the result of active anti-inflammatory processes (e.g., induction of beneficial T regulatory responses) that would not be elicited or perhaps would even be blocked in the setting of CS blockade, as well as attenuated inflammatory responses. Finally, CS blockade affects only adaptive immune responses, whereas the interface between innate immunity and SIV may be a key difference both in determining and maintaining the balance between beneficial and detrimental immune responses to SIV infection in natural and non-natural hosts.

Nevertheless, the experimental paradigm developed in this study will likely also be relevant to the analysis of other targeted immune interventions designed to probe the beneficial and detrimental determinants of AIDS virus infections in nonhuman primates. It is anticipated that such studies will enable a greater understanding of the mechanisms of AIDS pathogenesis and lead to the identification of immune interventions that successfully block deleterious effects of chronic immune activation without compromising beneficial host antiviral responses. The ultimate success of any such strategy will depend on the nature and specificity of the immunomodulatory intervention selected and the extent to which the SIV infection model chosen recapitulates the biology of HIV disease in humans.

Acknowledgments

This research was supported by NIH grants R01-AI49155-02 (to M.B. Feinberg), T32-AI07470 and T32-AI07442 (to D.A. Garber), P51 RR00165-42 (to Yerkes Primate Research Center), and P30 AI50409-04A1 (to Emory/Atlanta Center for AIDS Research). D.A. Garber is an Elizabeth Glaser Scholar of the Pediatric AIDS Foundation. The authors wish to acknowledge the contributions of the following people: Chris Ibegbu and Ashley Carter for assistance with flow cytometry, Lily Wang for providing tetramer reagents, Kirk Easley for assistance with statistical analyses, Diane Hollenbaugh (Bristol-Myers Squibb) for providing us with CTLA4-Ig and anti-CD40L mAb, David Watkins, Nancy Wilson and David Lorentzen (HLA/Molecular Diagnostics Laboratory, University of Wisconsin) for providing macaque MHC genotyping services, Stephanie Ehnert and Andrew Adams for providing expert animal handling and care, Dan Anderson for conducting macaque necropsies, Jeff Safrit and Robert Mittler for providing helpful discussions, and Kate Garber for critical reading of the manuscript.

Received for publication July 9, 2003, and accepted in revised form December 16, 2003.

Address correspondence to: Mark Feinberg, Emory Vaccine Center, 954 Gatewood Road, Atlanta, Georgia 30329, USA. Phone: (404) 727-4374; Fax: (404) 727-8199; E-mail: mbf@sph.emory.edu.

1. Koup, R.A., et al. 1994. Temporal association of cellular immune responses with the initial control of viremia in primary human immunodeficiency virus type 1 syndrome. *J. Virol.* **68**:4650–4655.
2. Borrow, P., Lewicki, H., Hahn, B.H., Shaw, G.M., and Oldstone, M.B. 1994. Virus-specific CD8+ cytotoxic T-lymphocyte activity associated with control of viremia in primary human immunodeficiency virus type 1 infection. *J. Virol.* **68**:6103–6110.
3. Reimann, K.A., et al. 1994. Immunopathogenic events in acute infection of rhesus monkeys with simian immunodeficiency virus of macaques. *J. Virol.* **68**:2362–2370.
4. Kuroda, M.J., et al. 1999. Emergence of CTL coincides with clearance of virus during primary simian immunodeficiency virus infection in rhesus monkeys. *J. Immunol.* **162**:5127–5133.
5. Mellors, J.W., et al. 1996. Prognosis in HIV-1 infection predicted by the quantity of virus in plasma. *Science.* **272**:1167–1170.
6. Hirsch, V.M., et al. 1996. Patterns of viral replication correlate with outcome in simian immunodeficiency virus (SIV)-infected macaques: effect of prior immunization with a trivalent SIV vaccine in modified vaccinia virus Ankara. *J. Virol.* **70**:3741–3752.
7. Watson, A., et al. 1997. Plasma viremia in macaques infected with simian immunodeficiency virus: plasma viral load early in infection predicts survival. *J. Virol.* **71**:284–290.
8. Staprans, S.I., et al. 1999. Simian immunodeficiency virus disease course is predicted by the extent of virus replication during primary infection. *J. Virol.* **73**:4829–4839.
9. Allen, T.M., et al. 2000. Tat-specific cytotoxic T lymphocytes select for SIV escape variants during resolution of primary viraemia. *Nature.* **407**:386–390.
10. Evans, D.T., et al. 1999. Virus-specific cytotoxic T-lymphocyte responses select for amino-acid variation in simian immunodeficiency virus Env and Nef. *Nat. Med.* **5**:1270–1276.
11. McMichael, A. 1998. T cell responses and viral escape. *Cell.* **93**:673–676.
12. Schmitz, J.E., et al. 1999. Control of viremia in simian immunodeficiency virus infection by CD8+ lymphocytes. *Science.* **283**:857–860.
13. Matano, T., et al. 1998. Administration of an anti-CD8 monoclonal antibody interferes with the clearance of chimeric simian/human immunodeficiency virus during primary infections of rhesus macaques. *J. Virol.* **72**:164–169.
14. Jin, X., et al. 1999. Dramatic rise in plasma viremia after CD8(+) T cell depletion in simian immunodeficiency virus-infected macaques. *J. Exp. Med.* **189**:991–998.
15. Kaur, A., Hale, C.L., Ramanujan, S., Jain, R.K., and Johnson, R.P. 2000. Differential dynamics of CD4(+) and CD8(+) T-lymphocyte proliferation and activation in acute simian immunodeficiency virus infection. *J. Virol.* **74**:8413–8424.
16. Phillips, A.N. 1996. Reduction of HIV concentration during acute infection: independence from a specific immune response. *Science.* **271**:497–499.
17. Linsley, P.S. 1991. CTLA-4 is a second receptor for the B cell activation antigen B7. *J. Exp. Med.* **174**:561–569.
18. Guermonprez, P., Valladeau, J., Zitvogel, L., Thery, C., and Amigorena, S. 2002. Antigen presentation and T cell stimulation by dendritic cells. *Annu. Rev. Immunol.* **20**:621–667.
19. Bennett, S.R., et al. 1998. Help for cytotoxic-T-cell responses is mediated by CD40 signalling. *Nature.* **393**:478–480.
20. Schoenberger, S.P., Toes, R.E., van der Voort, E.I., Offringa, R., and Melief, C.J. 1998. T-cell help for cytotoxic T lymphocytes is mediated by CD40-CD40L interactions. *Nature.* **393**:480–483.
21. Ridge, J.P., Di Rosa, F., and Matzinger, P. 1998. A conditioned dendritic cell can be a temporal bridge between a CD4+ T-helper and a T-killer cell. *Nature.* **393**:474–478.
22. Linsley, P.S., et al. 1992. Immunosuppression in vivo by a soluble form of the CTLA-4 T cell activation molecule. *Science.* **257**:792–795.
23. Wallace, P.M., Rodgers, J.N., Leytze, G.M., Johnson, J.S., and Linsley, P.S. 1995. Induction and reversal of long-lived specific unresponsiveness to a T-dependent antigen following CTLA4Ig treatment. *J. Immunol.* **154**:5885–5895.
24. Laman, J.D., Claassen, E., and Noelle, R.J. 1996. Functions of CD40 and its ligand, gp39 (CD40L). *Crit. Rev. Immunol.* **16**:59–108.
25. Bourgeois, C., Rocha, B., and Tanchot, C. 2002. A role for CD40 expression on CD8+ T cells in the generation of CD8+ T cell memory. *Science.* **297**:2060–2063.
26. Borrow, P., et al. 1998. CD40 ligand-mediated interactions are involved in the generation of memory

CD8(+) cytotoxic T lymphocytes (CTL) but are not required for the maintenance of CTL memory following virus infection. *J. Virol.* **72**:7440–7449.
27. Grewal, I.S., et al. 1996. Requirement for CD40 ligand in costimulation induction, T cell activation, and experimental allergic encephalomyelitis. *Science.* **273**:1864–1867.
28. Grewal, I.S., Xu, J., and Flavell, R.A. 1995. Impairment of antigen-specific T-cell priming in mice lacking CD40 ligand. *Nature.* **378**:617–620.
29. van Essen, D., Kikutani, H., and Gray, D. 1995. CD40 ligand-transduced co-stimulation of T cells in the development of helper function. *Nature.* **378**:620–623.
30. Yang, Y., and Wilson, J.M. 1996. CD40 ligand-dependent T cell activation: requirement of B7-CD28 signaling through CD40. *Science.* **273**:1862–1864.
31. Larsen, C.P., et al. 1996. Long-term acceptance of skin and cardiac allografts after blocking CD40 and CD28 pathways. *Nature.* **381**:434–438.
32. Kirk, A.D., et al. 1997. CTLA4-Ig and anti-CD40 ligand prevent renal allograft rejection in primates. *Proc. Natl. Acad. Sci. U. S. A.* **94**:8789–8794.
33. Adams, A.B., Pearson, T.C., and Larsen, C.P. 2001. Conventional immunosuppression and co-stimulation blockade. *Philos. Trans. R. Soc. Lond. B. Biol. Sci.* **356**:703–705.
34. Altman, J.D., et al. 1996. Phenotypic analysis of antigen-specific T lymphocytes. *Science.* **274**:94–96.
35. Allen, T.M., et al. 1998. Characterization of the peptide binding motif of a rhesus MHC class I molecule (Mamu-A*01) that binds an immunodominant CTL epitope from simian immunodeficiency virus. *J. Immunol.* **160**:6062–6071.
36. Mothe, B.R., et al. 2002. Dominance of CD8 responses specific for epitopes bound by a single major histocompatibility complex class I molecule during the acute phase of viral infection. *J. Virol.* **76**:875–884.
37. Miller, M.D., Yamamoto, H., Hughes, A.L., Watkins, D.I., and Letvin, N.L. 1991. Definition of an epitope and MHC class I molecule recognized by gag-specific cytotoxic T lymphocytes in SIVmac-infected rhesus monkeys. *J. Immunol.* **147**:320–329.
38. Knapp, L.A., Lehmann, E., Piekarczyk, M.S., Urvater, J.A., and Watkins, D.I. 1997. A high frequency of Mamu-A*01 in the rhesus macaque detected by polymerase chain reaction with sequence-specific primers and direct sequencing. *Tissue Antigens.* **50**:657–661.
39. Lewis, M.G., et al. 1994. Titration and characterization of two rhesus-derived SIVmac challenge stocks. *AIDS Res. Hum. Retroviruses.* **10**:213–220.
40. Hofmann-Lehmann, R., et al. 2000. Sensitive and robust one-tube real-time reverse transcriptase-polymerase chain reaction to quantify SIV RNA load: comparison of one- versus two-enzyme systems. *AIDS Res. Hum. Retroviruses.* **16**:1247–1257.
41. Amara, R.R., et al. 2001. Control of a mucosal challenge and prevention of AIDS by a multiprotein DNA/MVA vaccine. *Science.* **292**:69–74.
42. Montefiori, D.C., Baba, T.W., Li, A., Bilska, M., and Ruprecht, R.M. 1996. Neutralizing and infection-enhancing antibody responses do not correlate with the differential pathogenicity of SIVmac239delta3 in adult and infant rhesus monkeys. *J. Immunol.* **157**:5528–5535.
43. Ware, J.H. 1985. Linear models for the analysis of longitudinal studies. *The American Statistician.* **39**:95–101.
44. Murali-Krishna, K., et al. 1998. Counting antigen-specific CD8 T cells: a reevaluation of bystander activation during viral infection. *Immunity.* **8**:177–187.
45. Gerdes, J., et al. 1984. Cell cycle analysis of a cell proliferation-associated human nuclear antigen defined by the monoclonal antibody Ki-67. *J. Immunol.* **133**:1710–1715.
46. Pitcher, C.J., et al. 2002. Development and homeostasis of T cell memory in rhesus macaque. *J. Immunol.* **168**:29–43.
47. Mohri, H., et al. 2001. Increased turnover of T lymphocytes in HIV-1 infection and its reduction by antiretroviral therapy. *J. Exp. Med.* **194**:1277–1287.
48. O'Connor, D.H., et al. 2002. Acute phase cytotoxic T lymphocyte escape is a hallmark of simian immunodeficiency virus infection. *Nat. Med.* **8**:493–499.
49. Regoes, R.R., et al. 2004. The roles of target cells and virus-specific cellular immunity in primary SIV infection. *J. Virol.* In press.
50. Slavik, J.M., Hutchcroft, J.E., and Bierer, B.E. 1999. CD28/CTLA-4 and CD80/CD86 families: signaling and function. *Immunol. Res.* **19**:1–24.
51. Zajac, A.J., et al. 1998. Viral immune evasion due to persistence of activated T cells without effector function. *J. Exp. Med.* **188**:2205–2213.
52. Shedlock, D.J., and Shen, H. 2003. Requirement for CD4 T cell help in generating functional CD8 T cell memory. *Science.* **300**:337–339.
53. Sun, J.C., and Bevan, M.J. 2003. Defective CD8 T cell memory following acute infection without CD4 T cell help. *Science.* **300**:339–342.
54. Binley, J.M., et al. 1997. Differential regulation of the antibody responses to Gag and Env proteins of human immunodeficiency virus type 1. *J. Virol.* **71**:2799–2809.
55. Polacino, P.S., Liang, H.A., and Clark, E.A. 1995. Formation of simian immunodeficiency virus long terminal repeat circles in resting T cells requires both T cell receptor- and IL-2-dependent activation. *J. Exp. Med.* **182**:617–621.
56. Zhang, Z., et al. 1999. Sexual transmission and propagation of SIV and HIV in resting and activated CD4+ T cells. *Science.* **286**:1353–1357.
57. Haase, A.T. 1999. Population biology of HIV-1 infection: viral and CD4+ T cell demographics and dynamics in lymphatic tissues. *Annu. Rev. Immunol.* **17**:625–656.
58. Champagne, P., et al. 2001. Skewed maturation of memory HIV-specific CD8 T lymphocytes. *Nature.* **410**:106–111.
59. Wherry, E.J., Blattman, J.N., Murali-Krishna, K., van der Most, R., and Ahmed, R. 2003. Viral persistence alters CD8 T-cell immunodominance and tissue distribution and results in distinct stages of functional impairment. *J. Virol.* **77**:4911–4927.
60. Appay, V., et al. 2000. HIV-specific CD8(+) T cells produce antiviral cytokines but are impaired in cytolytic function. *J. Exp. Med.* **192**:63–75.
61. Vogel, T.U., Allen, T.M., Altman, J.D., and Watkins, D.I. 2001. Functional impairment of simian immunodeficiency virus-specific CD8+ T cells during the chronic phase of infection. *J. Virol.* **75**:2458–2461.
62. Kostense, S., et al. 2002. Persistent numbers of tetramer+ CD8(+) T cells, but loss of interferon-gamma+ HIV-specific T cells during progression to AIDS. *Blood.* **99**:2505–2511.
63. Ho, D.D., and Huang, Y. 2002. The HIV-1 vaccine race. *Cell.* **110**:135–138.
64. Douek, D.C., et al. 2002. HIV preferentially infects HIV-specific CD4+ T cells. *Nature.* **417**:95–98.
65. Perelson, A.S., Neumann, A.U., Markowitz, M., Leonard, J.M., and Ho, D.D. 1996. HIV-1 dynamics in vivo: virion clearance rate, infected cell life-span, and viral generation time. *Science.* **271**:1582–1586.
66. Forthal, D.N., Landucci, G., and Daar, E.S. 2001. Antibody from patients with acute human immunodeficiency virus (HIV) infection inhibits primary strains of HIV type 1 in the presence of natural-killer effector cells. *J. Virol.* **75**:6953–6961.
67. Montefiori, D.C., Graham, B.S., Zhou, J.Y., Zhou, J.T., and Ahearn, J.M. 1994. Binding of human immunodeficiency virus type 1 to the C3b/C4b receptor CR1 (CD35) and red blood cells in the presence of envelope-specific antibodies and complement. National Institutes of Health AIDS Vaccine Clinical Trials Networks. *J. Infect. Dis.* **170**:429–432.
68. Richman, D.D., Wrin, T., Little, S.J., and Petropoulos, C.J. 2003. Rapid evolution of the neutralizing antibody response to HIV type 1 infection. *Proc. Natl. Acad. Sci. U. S. A.* **100**:4144–4149.
69. McCune, J.M. 2001. The dynamics of CD4+ T-cell depletion in HIV disease. *Nature.* **410**:974–979.
70. Sousa, A.E., Carneiro, J., Meier-Schellersheim, M., Grossman, Z., and Victorino, R.M. 2002. CD4 T cell depletion is linked directly to immune activation in the pathogenesis of HIV-1 and HIV-2 but only indirectly to the viral load. *J. Immunol.* **169**:3400–3406.
71. Sopper, S., et al. 2003. Impact of simian immunodeficiency virus (SIV) infection on lymphocyte numbers and T-cell turnover in different organs of rhesus monkeys. *Blood.* **101**:1213–1219.
72. Hazenberg, M.D., Hamann, D., Schuitemaker, H., and Miedema, F. 2000. T cell depletion in HIV-1 infection: how CD4+ T cells go out of stock. *Nat. Immunol.* **1**:285–289.
73. Grossman, Z., Meier-Schellersheim, M., Sousa, A.E., Victorino, R.M., and Paul, W.E. 2002. CD4+ T-cell depletion in HIV infection: are we closer to understanding the cause? *Nat. Med.* **8**:319–323.
74. Silvestri, G., et al. 2003. Nonpathogenic SIV infection of sooty mangabeys is characterized by limited bystander immunopathology despite chronic high-level viremia. *Immunity.* **18**:441–452.
75. Silvestri, G., and Feinberg, M.B. 2003. Turnover of lymphocytes and conceptual paradigms in HIV infection. *J. Clin. Invest.* **112**:821–824. doi:10.1172/JCI200319799.